Adapting the Budyko Model to Analyze Permafrost Recession and Potential for Carbon Feedback

John Nguyen and Aileen Zebrowski

November 25, 2020

Abstract

Permafrost is a thick layer of soil that is frozen throughout the year and covers significant portions of the northern hemisphere. Currently, there is a large amount of carbon trapped in the permafrost, and as permafrost melts, a significant portion of this carbon will be released into the atmosphere as either carbon dioxide or methane. We use empirical data to estimate that, on average, permafrost currently extends from the arctic to latitude 61°N. We propose an adaption to the Budyko energy balance model to study the impacts of receding permafrost. We track the steady-state latitude of both the permafrost line and the snow line as greenhouse gas emissions, and consequently, global mean temperature increases. Using the change in permafrost surface area, we are able to quantify the total carbon feedback of melting permafrost. Focusing our analysis on scenarios described in recent IPCC reports and the Paris Climate Agreement, we use change in the permafrost line latitude to estimate the amount of carbon dioxide released by the melted permafrost. Similarly, we use the snow line to calculate the minimum average global temperature that would cause the ice caps to completely melt. We find that our adaption of the Budyko model produces estimates of carbon dioxide emissions within the range of projections of models with higher complexity.

Introduction

Permafrost is a layer of frozen soil that exists when temperatures remain at or below freezing for at least two years in a row. Primarily located in the arctic regions and the alpine and polar tundra, permafrost composes up to 24% of the northern hemisphere. Permafrost depth can range from a few centimeters to over 1,650 meters deep [1]. Due to an increase in global mean temperature, the permafrost has begun to melt. The goal of our adaption of the Budyko energy balance model is to assess the degree to which these temperature changes will cause a northward recession of the permafrost boundary. This is done using a number of scenarios that describe the state of the climate under possible future conditions. The IPCC (Intergovernmental Panel on Climate Change) has published several scenarios, each accounting for varying amounts of global cooperation [2], which we apply to our adapted model. In April 2016, the Paris Agreement was signed by 195 countries to attempt to prevent global mean temperature from increasing by more than 2°C [3]. The results of applying the Paris Agreement and the IPCC scenarios are analyzed and compared below. In this paper we also consider another scenario, which we dub 70N, as the climate state in which the permafrost line recedes to 70°N. These different scenarios provide context for permafrost recession.

1

From the IPCC and Paris Agreement, we focus on several particular scenarios. We consider the B1, A1T/B2, A1B, A2, and A1FI IPCC projections from the IPCC Fourth Assessment Report [2]. These projections describe the state of the climate in 2050 using various metrics such as annual carbon emissions and global mean temperature. The A1 scenarios describe a world with rapid economic growth and a globally integrated economy. The A2 scenario assumes high population growth and low economic growth. The B1 projections describe a world similar to A1, but with even more rapid growth. Similarly, the B2 scenario describes a world with intermediate economic and population growth. We group A1T and B2 together because they are both projected to increase global mean temperature by 2.4°C in the IPCC Fourth Assessment Report. A1T is a scenario from the A1 branch which emphasises the use of non-fossil fuel energy sources. The A1B scenario assumes there is a balance of fossil-fuel energy sources and non-fossil fuel sources. The A1FI scenario assumes fossil fuels are still the primary source of energy. The Paris Agreement includes two scenarios: ParisA and ParisB. The ParisA scenario describes the optimistic goal of limiting the global temperature increase below 1.5°C. The ParisB scenario limits the temperature increase to 2°C. The final scenario, 70N, is when the permafrost line reaches 70N latitude. We use this extreme scenario as a reference to interpret our results.

Incoming solar radiation (insolation) drives the climate system by supplying heat and energy to the Earth. Some insolation is reflected by the Earth's surface, and a fraction of this surface radiation is captured by greenhouse gases such as carbon dioxide and methane. Industrialization and the burning of fossil fuels has led to higher concentrations of greenhouse gases in the atmosphere causing global mean temperature to increase. The increasing temperatures cause regions that were once covered in permafrost to become too warm for soil to freeze year-round. As a result, frozen organic material begins to decay, releasing more greenhouse gases into the atmosphere. This cycle creates a number of consequences. For instance, Schuur et al. noted how an increase in global temperature could create a longer growing season [4]. Gruber and Haeberli studied melting permafrost in bedrock, and the potential for fracturing [5]. In this work, we examine the relationship between increasing global mean temperatures and the latitude of the permafrost and snow lines, and the carbon stored therein. While other literature uses 'ice line' in the place of 'snow line', we use 'snow line' in this paper to avoid confusion about the difference between 'ice' and 'permafrost'.

We focus our analysis on quantifying the amount of carbon dioxide released by melting permafrost. Melting permafrost releases mostly carbon dioxide and some methane [6]. The "perturbation lifetime" of a gas is the amount of time needed for a gas to decompose to 37% of the original amount. The perturbation lifetime of methane is approximately 12 years [7]. Since we are considering equilibrium solutions, 12 years is a short timespan. Furthermore, according to Hope and Schaefer, only 2.3% of total carbon emissions from permafrost is expected to be methane [8]. For this reason, we will assume all gases released by melting permafrost is carbon dioxide. Carbon dioxide enters permafrost from buried terrestrial vegetation that is frozen over. This vegetation could be encased in ice for thousands of years, and it decomposes into carbon dioxide, among other products [9].

First, we introduce the Budyko Model. Then, in the Model Formulation section, we adapt the Budyko model into a model which calculates the amount of permafrost melted given global mean temperature. Increases in atmospheric carbon prevents more radiation from escaping, caus-

ing a surplus of energy on Earth. According to the Budyko model, this imbalance will be fixed by increasing global mean temperature and therefore northward movement of the permafrost line. Currently, permafrost extends southward to about 61°N latitude, which we call the "permafrost line". We apply our adapted model to the IPCC projections, Paris Agreement, and 70N to calculate the position the permafrost line will stabilize to. Therefore, we can determine the surface area of melted permafrost and calculate how much sequestered carbon was released. We then chart the permafrost line and snow line with respect to increasing global mean temperature to visualize the impact of receding permafrost.

Budyko Model

The Budyko energy balance model compares the amount of energy absorbed by the Earth from the Sun with the amount of energy the Earth radiates outwards [10]. Any imbalance causes a change in global mean temperature. The main idea of the Budyko energy balance model is to explore how energy reflected by ice or ocean affects global mean temperature. As solar radiation enters the atmosphere, part of it is reflected by the surface. Surface ice and snow are more reflective (has a higher albedo) than other surfaces, e.g. land, trees, or ocean. The total energy the planet absorbs is the amount of incoming energy minus the amount of reflected energy that escapes the atmosphere. We define the snow line as the latitude where the ice line condition, detailed in [11], is satisfied. Using this model, we can derive the global mean temperature, and use that to determine the equilibrium snow and permafrost line position. We can simulate this phenomenon with the Budyko model by increasing global mean temperature and observing change in the snow and permafrost lines.

The Budyko model is given by the partial differential equation [12]:

$$R\frac{\partial T}{\partial t} = Qs(y) - Qs(y)\alpha(\eta, y) - (A + BT(y,t)) - C(\overline{T}(t) - T(y,t)) \tag{1}$$

which represents the instantaneous rate of change of temperature due to the balance of incoming and outgoing energy on the surface of the Earth [13]. Tung uses η to represent the sine of the permafrost line latitudinal position. We will use θ_p in a similar manner to represent the sine of the permafrost line position. Note that in Tung's description of the Budyko model, η is dynamic, while we allow θ_p to instantaneously jump to a new position given global mean temperature. Here, y is the independent variable, representing the sine of the latitude we want to observe. For definitions of variables and parameters values, see Table 1.

The term $Qs(y)$ represents the distribution of insolation across the planet, where Q is the solar constant and $s(y)$ is a function representing the distribution of insolation over the Earth; it incorporates the obliquity of the planet's rotation. Obliquity is the axial tilt of the planet's rotation. Insolation is shorthand for incoming solar radiation; it is a measure of how much sunlight the Earth receives at some latitude y. In contrast, the reflection term $Qs(y)\alpha(\eta, y)$ represents the amount of radiation reflected by planet, back into space. The α term is the albedo of the planet surface, given by:

Item	Value	Units	Meaning
Variables			
t		yr	Time
y	-	-	Sine of latitude
$T(t,y)$		°C	Surface temperature
Parameters			
θ_{p0}	61	°N	Initial permafrost line latitude
R	-	W yr/(m^2 °C)	Planetary heat capacity
Q	343	W/m^2	Insolation (incoming solar radiation)
s_2	-0.482	-	Estimation of the effect of obliquity on insolation [14]
α_1	0.32	-	Albedo for latitudes south of the snow line
α_2	0.62	-	Albedo for latitudes north of the snow line
A	202	W/m^2	Temperature-independent outgoing longwave radiation
B	1.90	W/(m^2 °C)	Temperature-dependent outgoing longwave radiation
C	3.04	W/(m^2 °C)	Heat transport coefficient
T_c	-10	°C	Critical temperature at the snow line

Table 1: Variables and parameters in the Budyko energy balance model. All parameter values are as in [13]. Note that η is calculating using $T(t,y)$.

$$\alpha = \begin{cases} \alpha_1 & y \leq \eta \\ \alpha_2 & y > \eta \end{cases}$$

We refer to the proportion of radiation reflected by the surface as albedo. Here, α_1 represents ocean albedo, α_2 represents ice cap albedo and η represents the sine of the latitude of the snow line. Since the Earth's surface is 70% water, we assume the surface is either water or ice. The outgoing longwave radiation term, $(A + BT)$, describes the amount of radiation trapped in the atmosphere. The transport term, $C(\overline{T} - T)$, represents heat transport from differential heating of the Earth's surface and the consequential mixing through air and ocean currents from nearby regions. Notice that this term is derived from Netwon's Law of Cooling which causes temperatures to relax towards the mean temperature. Here, the global mean temperature, $\overline{T}$, is the average annual temperature of the Earth surface. In our analysis, we vary this term to determine how the resulting permafrost and snow line locations change.

We utilize a quadratic approximation of the distribution of insolation, $s(y)$, provided by McGehee and Widiasih [12] in order to map the snow line location, taking into account the change in albedo and temperature with respect to latitude.

The steady-state temperature of (1) is given by [15]:

$$T(y) = \frac{1}{B + C} \left(Qs(y)(1 - \alpha(\eta, y)) - A + C\overline{T} \right) \tag{2}$$

Here, $\overline{T}$ is global mean temperature at equilibrium and $T(y)$ is temperature at latitude x, where $y = \sin(\theta)$ and steady-state snow line position η. We adapt the quadratic approximation to determine changes in global mean temperature and permafrost line location. With this new temperature distribution, we can adapt the Budyko model to determine the new position of the permafrost line under conditions described by various scenarios.

Formulation of Adapted Model

In this section, we define the relevant variables we use to formulate our adapted model. Let $T(y)$ represent the temperature at $y = \sin(\theta)$, where θ is the latitude, and the permafrost line is at latitude θ_p. To make calculating the latitude of the permafrost line simpler, we substitute $p = \sin(\theta_p)$ in our equations. We define the permafrost line to be the latitude θ_p such that:

$$T(p) = \frac{1}{B+C} \left(Qs(p)(1-\alpha_1) - A + C\overline{T} \right) = 0 \tag{3}$$

Recall that Q is the solar constant, and the function $s(y)$ is the latitudinal distribution function calculated as a Fourier-Legendre series using the Earth's obliquity [15]. So in the above formula, $s(p)$ represents the the proportion of sunlight recieved at the permafrost line.

To determine changes in the permafrost line, we take the derivative of this temperature function with respect to global mean temperature, $\overline{T}$, and then solve for the derivative of the latitude of the permafrost line, $\frac{dp}{d(\overline{T})}$. Notice that p is a function of $T(y)$, so we will be computing $\frac{dp}{dT}$, which we will reference as p' henceforth. From there, we will take the arcsine to solve for the position of the permafrost line. We start with the derivative of the temperature, as follows:

$$\frac{dT(p)}{d(\overline{T})} = \frac{dT(p)}{dp} \frac{dp}{d(\overline{T})} \tag{4}$$

We can find the equilibrium solution by setting the derivative to zero:

$$\frac{dT(p)}{d(\overline{T})} = \frac{1}{B+C} \left(Q \frac{d}{d(\overline{T})} \left(\frac{ds(p(\overline{T}))}{dp(\overline{T})} \right)(1-\alpha_1) + C \right) = 0 \tag{5}$$

By simplifying, we obtain the following formula:

$$Qs'(p(\overline{T}))p'(\overline{T})(1-\alpha_1) + C = 0. \tag{6}$$

We now apply a quadratic approximation of the distribution function, $s(p)$, introduced by North [15]. This approximates the insolation at the permafrost line:

$$s(p) = 1 + s_2 \left(\frac{1}{2}(3p^2 - 1) \right)$$

Rearranging (6) to find the equilibrium solution of $p'(\overline{T})$:

$$p'(\overline{T}) = \frac{-C}{Qs'(p(\overline{T}))(1 - \alpha_1)} \tag{7}$$

Plugging in the quadratic approximation $s(p)$, we find:

$$p'(\overline{T}) = \frac{-C}{3Qs_2 p(\overline{T})(1 - \alpha_1)} \tag{8}$$

Taking a discrete approximation to the derivative, we are able to formulate an equation for the permafrost line with respect to global mean temperature:

$$\Delta\theta_p = \arcsin(\Delta p) = \frac{1}{\sqrt{1 - (\sin^2 \theta_{p0})}} p'(\overline{T})\Delta\overline{T} \tag{9}$$

Note that the equilibria of (8) can be solved explicitly and are satisfied by $p_1 \approx 0.1$ and $p_2 \approx 0.9$. Two other physically attainable states are when $p = 1$, which represents an ice-free planet, and $p = 0$, which represents an ice-covered planet.

To begin to analyze the recession of the permafrost line, we must estimate the current position of the permafrost line. Most of the world's permafrost exists in the northern hemisphere due to higher non-glaciated land area there compared to the southern hemisphere. The permafrost in the northern circum-polar region is shown in Figure 2. By considering the lowest latitude at which permafrost occurs for each longitude, we obtain an average current permafrost line at 61°N, which we visualize in blue on Figure 2. There are four categories of permafrost: continuous, discontinuous, sporadic and isolated. In Figure 2, the green in the figure represents continuous and discontinuous permafrost from data collected in [16]. These regions were categorized by Brown et al. by the percentage of land that is covered by permafrost within the area [16]. They are defined as $90\% - 100\%$ (continuous), $50\% - 90\%$ (discontinuous), $10\% - 50\%$ (sporadic) and $< 10\%$ (isolated). In our model, we only consider continuous and discontinuous permafrost. The carbon lost by not considering these less concentrated permafrost regions is assumed to be compensated for by treating the discontinuous permafrost regions as continuous, and assuming carbon within permafrost is evenly distributed throughout the area.
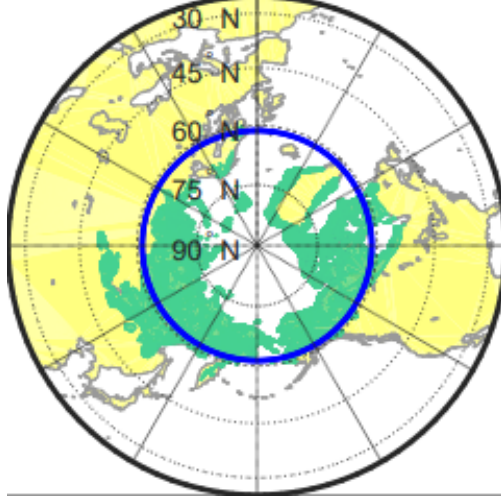
Figure 2: Diagram of continuous and discontinuous permafrost (green) with the average permafrost latitude charted. Permafrost data used can be found in [16].

Let $\Delta\theta_p$ be the change in permafrost latitude. Using $\Delta\theta_p$, we calculate a corresponding change in permafrost surface area, ΔSA_p. To do this, we calculate Earth's surface area (SA_E) between the original and adjusted permafrost line latitude using the difference of spherical caps of the same sphere:

$$\Delta SA_E = 2\pi r^2(\sin(\theta_p) - \sin(\theta_{p0})) \tag{10}$$

Note that we use sine instead of cosine because latitude is the inside angle between the North Pole and the equator, while the standard spherical cap formula uses the outside angle.

Let θ_{p0} and θ_p are the initial latitude and final latitude of permafrost, respectively. Thus if the model predicts the permafrost line will change by $\Delta\theta$, then $\theta_p = \theta_{p0} - \Delta\theta$. The radius of the Earth is $r = 6371$ km. Currently, permafrost covers approximately $1 - \cos 61°$ of the Earth's surface area. Using 10, we derive our function to compute change in permafrost:

$$\Delta SA_p = 2.55 \times 10^{14}\left(\sin\left(61° + \Delta\theta_p\right) - \sin 61°\right), \tag{11}$$

There is about 1672 Gt of carbon sequestered in permafrost [17]. Assuming this is evenly distributed throughout the entire permafrost area, the carbon emissions are directly proportional to the area lost. Thus we project total carbon emissions from melting permafrost under the conditions described in the scenarios studied as:

$$\text{Carbon emissions} = (\text{Total Carbon in Permafrost})\left(\frac{\text{Change in Permafrost Surface Area}}{\text{Original Permafrost Surface Area}}\right)$$

Plugging in known values, we obtain:

$$(1672)\frac{\Delta SA_p}{1.32 \times 10^{13}}\text{ Gt} \tag{12}$$

In Table 3, the total carbon emissions is labelled as Sequestered Carbon Thawed. Recall the atomic weight of a carbon atom is 12.0107 amu, while the weight of a CO_2 molecule is 44.01 amu.

	ΔT (°C)	$\Delta\theta_p$ (°N)	Permafrost melt (million sq. km)	Permafrost loss (%)	Sequestered carbon thawed (Gigatons)	CO_2 emissions (Gigatons)	Emissions increase from current CO_2 levels (%)
IPCC Scenarios							
B1	1.8	2.2	4.6	3.5	58.1	213.0	14.1
A1T/B2	2.4	2.9	6.0	4.6	76.6	280.6	18.6
A1B	2.8	3.4	7.0	5.3	88.6	324.8	21.5
A2	3.4	4.1	8.4	6.4	106.3	389.5	25.8
A1FI	4.0	4.9	9.7	7.4	123.5	452.6	30.0
Other Scenarios							
ParisA	1.5	1.8	3.8	2.9	48.7	178.6	11.8
ParisB	2.0	2.4	5.1	3.8	64.3	235.7	15.6
70N	7.4	9.0	16.6	12.6	211.2	773.9	51.3

Table 3: Temperature change scenarios and the corresponding permafrost line recession and CO_2 release. CO_2 emissions calculated using (12). The first two columns are scenario names and the projected total mean temperature change. All other columns are from our adapted model. Emissions increase is relative to ESRL published data [18].

Thus we are able to calculate the total amount of CO_2 released by melting permafrost, which is labelled as CO_2 emissions in Table 3.

Results from the Adapted Model

In this section we compute the change in permafrost line latitude using (11) with the parameters in Table 1 and various projection estimates for global temperature change. Our results are summarized in Table 3.

Result 1. Carbon Emission Estimate

In the first column of Table 3, the first group of scenarios are those cited in the IPCC Fourth Assessment Report [2]; the Paris A and Paris B scenarios are goals stated in the Paris Agreement [3]; and the 70N scenario calculates the change in temperature corresponding to the recession of permafrost to 70°N latitude. The global mean temperature change, ΔT, is the expected temperature change in 2090-2099 relative to 1980-1999. For the IPCC and Paris scenarios, these temperature values were given in their respective documents [2, 3]. For the 70N scenario, we calculated the change in global mean temperature that would move our initial permafrost line at 61°N to 70°N. We calculate the change in the permafrost line, $\Delta\eta$ as a linear approximation, relative to the initial position 61°N. $\Delta\theta_p$ was calculated using (9). Using $\Delta\theta_p$, we calculate surface area of melted permafrost using (11). Using the change in surface area, we estimate the total atomic mass of

thawed sequestered carbon atoms using Formula 12. The CO_2 emissions column reports the total atomic mass of all carbon dioxide released based on our assumptions. The final column states the increase in atmospheric carbon dioxide relative to 2019 from data published by Earth Systems Research Laboratories. As of 2019, the average amount of carbon in the atmosphere is 411.33 ppm, or approximately 876.3 Gt C [18].

On April 22, 2016, 195 countries signed the Paris Agreement with the intention of preventing global mean temperature from increasing by more than 2°C, with a strong aim at keeping it below 1.5°C [3]. Relative to other projections, the Paris Agreement is an optimistic goal. In contrast, the 70N scenario is used as an estimate for near total permafrost loss since the vast majority of permafrost is south of this line. Our model predicts that a 5.4°C increase is necessary for the 70N scenario. Results for every scenario can be found in Table 3. Due to the linear nature of our approximation, the adapted Budyko energy balance model becomes less valid the farther away from starting temperature we go; however, we may use it as a first approximation to determine the likelihood of all permafrost melting.

Result 2. Climate Feedback Analysis

Recall that in the Budyko model, the parameter A is a measure of the temperature-independent outgoing longwave radiation (OLR) reflected by Earth. As greenhouse gases increase, OLR becomes trapped in the atmosphere, causing total radiation reflected by Earth to decrease. Consequently, the total energy absorbed by Earth increases [19]. We can simulate the greenhouse gas effect by decreasing A, representing how more energy is trapped beneath the atmosphere. We simulate this phenomena in Figure 3a.

By decreasing the parameter A, we can simulate a stronger greenhouse gas effect. Figure 3a shows the relationship between A and global mean temperature. The Paris Climate Agreement [3] was signed when global mean temperature was approximately 13°C, and tries to limit global mean temperature at 15°C. We notice the curve in this diagram is almost linear: on this diagram, if A increases by 2 units, the global mean temperature also increases by 2°C. In the model, the variable A describes how much sunlight escapes the Earth's atmosphere.

In Figure 3c, we plot the bifurcation diagram of the Budyko model using the above parameters. Notice for most values of A, when a solution to the snow and permafrost lines exist, the snow line is usually above the permafrost line. Furthermore, there is a saddle node bifurcation beyond which the snow line has no solutions, but the permafrost still does for some higher values of A. When the snow line and permafrost line bifurcation diagrams disappear, it represents the physical boundaries of the system.

We plot the snow line and permafrost line with respect to global mean temperature in Figure 3d. This gives us a tangible representation of how climate change directly effects the permafrost line. Notice that once global mean temperature reaches about 16.2°C the equilibrium solution of the snow line is at 90°, so we have no snow caps. Note that our model determines the steady state position of the permafrost and snow lines. While practically, there could be a dynamic recession of the permafrost and snow lines spanning hundreds or thousands of years, our analysis assumes
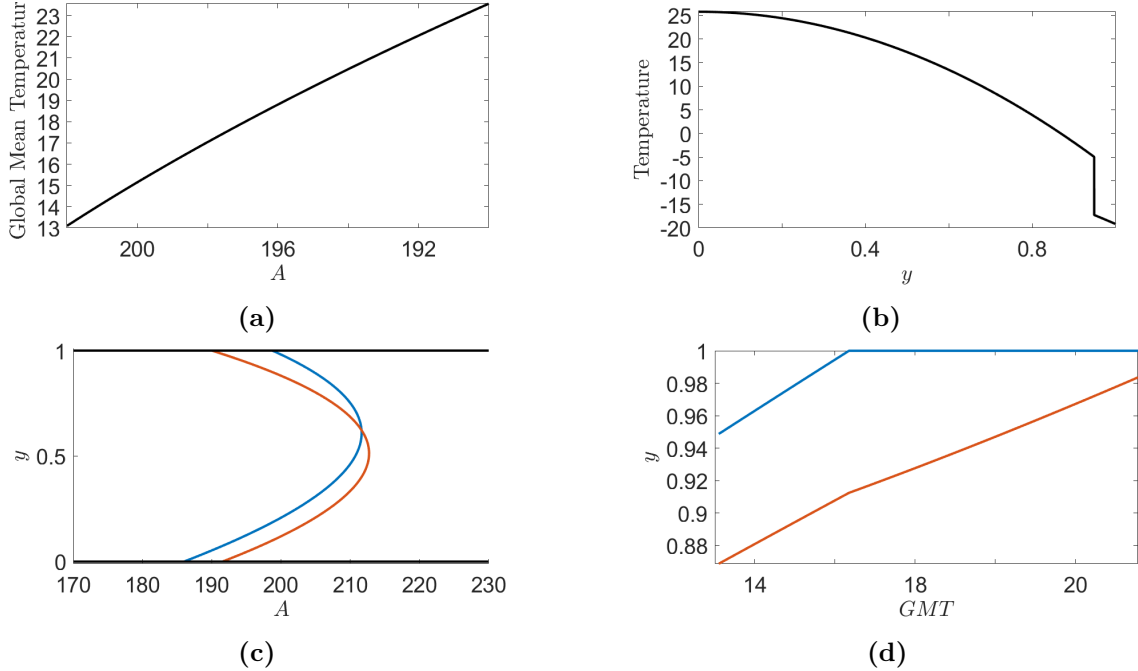
Figure 3: (a) Global mean temperature as a function of A for the equilibrium permafrost line, given by (3). (b) Annual mean temperature as a function of the sine of latitude. Figure is given by (2). (c) Sine of the equilibrium latitude of the permafrost line (orange) and snow line (blue) as a function of A. Figure is given by (3). (d) Sine of the equilibrium latitude of the snow line and permafrost line as a function of global mean temperature. Figure can be derived from (3).

there is an instantaneous response.

In Figure 3b, we show the current average annual temperature distribution of the Earth relative to the sine of the latitude. The large dip in temperature occurs at the snow line, which is currently $\sin \eta \approx 0.95$. The vertical line from $-5°C$ to $-17°C$ represent the temperature thresholds required to maintain year-round permafrost and year-round ice. So below the vertical line, we have year-round ice.

Result 3. Total Emission Estimate is within 95% Confidence Interval

Other estimates exist for the carbon emissions expected from the permafrost. Hope and Schaefer [8] made an estimate using the A1B scenario, shown in Figure 5b. This data is under the assumption that anthropogenic emissions cease in 2100, thereby allowing equilibrium to reestablish in the following 100 years. Given that our predictions are assuming equilibrium is reached, the estimate for the total CO_2 emissions under A1B from 2010 to 2200 would be directly comparable to the CO_2 emissions from this model using the A1B projection of $2.8°C$ increase. A first approximation of the total emissions given by Figure 5 can be found using the trapezoidal rule. We discretize the plot into a finite number of points on the curve. Let the nth point be (x_n, y_n). We use these points to approximate the area under the curve:
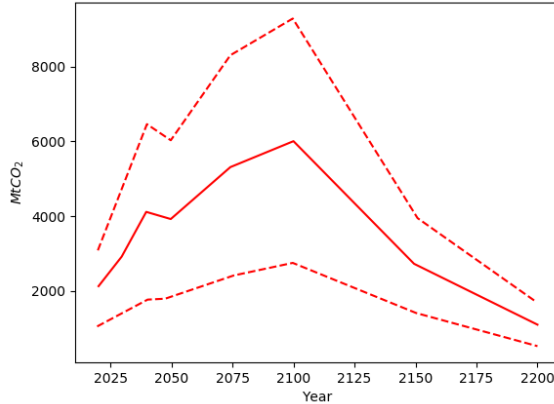
Figure 5: Estimated annual emissions of CO_2 from thawing permafrost for the A1B scenario from the IPCC AR4. The solid line shows the mean values and the dashed lines are the 5 and 95% confidence intervals.Reprinted by permission from Springer: Nature Climate Change [8], 2015.

$$\text{Total emissions} = \sum_{i=1}^{N} \frac{y_i + y_{i+1}}{2} \Delta x$$
$$= 687486.82 \text{ MtCO}_2$$
$$= 687 \text{ GtCO}_2$$

The total emissions of 687 Gt CO_2 is the best estimate provided, with a confidence interval between 320.25 and 1048.22 Gt CO_2 and therefore is within a 95% confidence interval [8]. Our model's prediction of 324.8 Gt CO_2 is on the low end, but still within the confidence interval.

One possible reason for this discrepancy could be that permafrost thickness changes with latitude. Our adapted model assumes an even permafrost distribution north of 61°C, however permafrost increases thickness with latitude which can be significant [8]. According to the assumptions used in our model, considering the discontinuous permafrost to be continuous is compensated for by neglecting regions of isolated and sporadic permafrost. Additionally, according to Figure 5, equilibrium has not been reached even by 2200. Additional carbon emissions in the following years trends towards our estimate.

Schaefer et al. provides a summary of many different model predictions for carbon emissions through 2200. For the IPCC A2 scenario the carbon emission predictions range from 46 to 435 Gt C, compared to 389.5 Gt C predicted by our model [20]. For reference, there is about 730 Gt C in the atmosphere currently [21]. This suggests there is the potential for significant carbon emissions from melting permafrost.

The various scenarios, excluding 70N, project a range from a 1.5°C to 4.0°C increase in the next 80 years. Using this temperature range, the model predicts between 1.2 and 2.6 million square

kilometers of permafrost melted and 18% to 48% increase in carbon in the atmosphere from current levels due to just permafrost. Therefore this may be a significant source of greenhouse gas emissions in the near future resulting in a strong positive feedback. This also stresses the importance of the Paris Agreement in maintaining manageable global CO_2 levels to minimize such positive feedback loops from reaching a tipping point.

Conclusion

We have discussed the impact of permafrost on climate change. Furthermore, we referenced several climate scenarios and calculated the amount of carbon released by the associated melting of permafrost. In particular, we analyzed the feedback loop wherein warming global temperatures and the consequential melting permafrost exacerbate climate change. Our analysis demonstrates where the snow and permafrost lines will recede to given change in global mean temperature. By projecting the amount of sequestered carbon released by melting permafrost according to different scenarios, we analyzed the relationship between carbon in the atmosphere and permafrost.

According to our adapted model, even the most optimistic projections, such as Paris A and B1, melting permafrost will have a non-trivial contribution to carbon in the atmosphere. Since we analyze the steady-state of the permafrost line, our model assumes the permafrost line instantly jumps in response to increasing global mean temperature. In reality, even if carbon emissions were to suddenly decrease, the permafrost line and snow line will continue to recede for many years until they converge to equilibrium.

Acknowledgements

References

[1] "National snow and ice data center." https://nsidc.org/cryosphere/frozenground/how_fg_forms.html.

[2] IPCC, M. L. Parry, O. F. Canziani, J. P. Palutikof, P. van der Linden, and C. E. Hanson, *IPCC Fourth Assessment Report: Working Group II Report "Impacts, Adaptation and Vulnerability"*. 01 2007.

[3] *Paris Agreement to the United Nations Framework Convention on Climate Change.* Dec. 12, 2015, T.I.A.S. No. 16-1104.

[4] E. A. G. Schuur, A. D. McGuire, C. Schädel, G. Grosse, J. W. Harden, D. J. Hayes, G. Hugelius, C. D. Koven, P. Kuhry, D. M. Lawrence, S. M. Natali, D. Olefeldt, V. E. Romanovsky,

K. Schaefer, M. R. Turetsky, C. C. Treat, and J. E. Vonk, "Climate change and the permafrost carbon feedback," *Nature*, vol. 520, pp. 171–179, Apr 2015.

[5] S. Gruber and W. Haeberli, "Permafrost in steep bedrock slopes and its temperaturerelated destabilization following climate change," *Journal of Geophysical Research: Earth Surface*, vol. 112, Jun 2007.

[6] E. A. Schuur, J. Bockheim, J. G. Canadell, E. Euskirchen, C. B. Field, S. V. Goryachkin, S. Hagemann, P. Kuhry, P. M. Lafleur, H. Lee, *et al.*, "Vulnerability of permafrost carbon to climate change: Implications for the global carbon cycle," *AIBS Bulletin*, vol. 58, no. 8, pp. 701–714, 2008.

[7] S. Solomon, D. Qin, M. Manning, Z. Chen, M. Marquis, K. B. Averyt, M. Tignor, H. L. Miller, *et al.*, "Ipcc, 2007. climate change: The physical science basis, year=2007, publisher=Cambridge University Press, New York, NY, USA,"

[8] C. Hope and K. Schaefer, "Economic impacts of carbon dioxide and methane released from thawing permafrost," *Nature*, vol. 6, 2016.

[9] L. Guo, C.-L. Ping, and R. W. Macdonald, "Mobilization pathways of organic carbon from permafrost to arctic rivers in a changing climate," *Geophys. Res. Lett*, vol. 34, 07 2007.

[10] M. I. Budyko, "The effect of solar radiation variations on the climate of the earth," *Tellus*, vol. 21, no. 5, pp. 611–619, 1969.

[11] E. R. Widiasih, "Dynamics of the budyko energy balance model," *SIAM Journal on Applied Dynamical Systems*, vol. 12, no. 4, pp. 2068–2092, 2013.

[12] R. McGehee and E. Widiasih, "A quadratic approximation of budyko's ice-albedo feedback model with ice line dynamics," *SIAM Journal of Applied Dynamical Systems*, vol. 13, 2014.

[13] K. K. Tung, *Topics in mathematical modeling*. Princeton, N.J. : Princeton University Press, 2007.

[14] P. Chylek and J. A. Coakley, "Analytical analysis of a budyko-type climate model," 1975.

[15] G. North, "Analytical solution to a simple climate model with diffusive heat transport," *Journal of the Atmospheric Sciences*, vol. 32, no. 7, pp. 1301–1307, 1975.

[16] J. Brown, O. Ferrians Jr, J. Heginbottom, and E. Melnikov, *Circum-Arctic map of permafrost and ground-ice conditions*. US Geological Survey, Reston, VA, 1997.

[17] C. Tarncai, J. G. Canadell, E. A. G. Schuur, P. Kuhry, G. Mazhitova, and S. Zimov, "Soil organic pools in the northern circumpolar permafrost region," *Global Biochemical Cycles*, vol. 23.

[18] P. Tans and R. Kneeling, "Global monitoring laboratory - carbon cycle greenhouse gases," Oct 2005.

[19] R. Pierrehumbert, *Principles of planetary climate*. Cambridge University Press, 2010.

[20] K. Schaefer, H. Lantuit, V. Romanovsky, E. Schuur, and R. Witt, "The impact of the permafrost carbon feedback on global climate," *Environmental Research Letters*, vol. 9, 2014.

[21] S. A. Zimov, E. A. Schuur, and F. S. Chapin III, "Permafrost and the global carbon budget," *Science*, vol. 312, no. 5780, pp. 1612–1613, 2006.